J Biomol NMR (2007) 39:239–245
DOI 10.1007/s10858-007-9192-4

ARTICLE

Hadamard NMR spectroscopy for relaxation measurements of large (>35 kDa) proteins

B. Tom Burnley · Arnout P. Kalverda · Stephen J. Paisey · Alan Berry · Steve W. Homans

Received: 24 July 2007 / Accepted: 31 August 2007 / Published online: 20 September 2007
© Springer Science+Business Media B.V. 2007

Abstract Here we present a suite of pulse sequences for the measurement of ^{15}N T_1, $T_{1\rho}$ and NOE data that combine traditional TROSY-based pulse sequences with band-selective Hadamard frequency encoding. The additive nature of the Hadamard matrix produces much reduced resonance overlap without the need for an increase in the dimensionality of the experiment or a significant decrease in the signal to noise ratio. We validate the accuracy of these sequences in application to ubiquitin and demonstrate their utility for relaxation measurements in *Escherichia coli* Class II fructose 1,6-bisphosphate aldolase (FBP-aldolase), a 358 residue 78 kDa dimeric enzyme.

Introduction

Protein dynamics are essential for function (Eisenmesser et al. 2005), and NMR relaxation experiments have provided quantitative sub-nanosecond dynamic information for over 280 protein systems (Jarymowycz and Stone 2006). However, larger protein systems offer a significant challenge. Indeed, at present there are very few examples of fully quantified backbone dynamic information for protomers greater than 25 kDa. Despite recent advances such as the development of TROSY-based pulse sequences (Pervushin et al. 1997) and the use of perdeuterated samples (Venters et al. 1996) allowing high quality spectra to be generated from large proteins, relaxation studies are limited by extensive cross-peak overlap in 2D ^{1}H–^{15}N correlation spectra.

As the number of residues in the polypeptide backbone increases, so does the potential for spectral overlap in the 2D ^{1}H–^{15}N HSQC spectra from which relaxation data are measured. Relaxation data from overlapping resonances cannot readily be analysed and therefore are typically excluded. Two recent approaches to improve this situation involve the acquisition of tilted projection planes (Tugarinov et al. 2004) or the use of a two point estimation of the relaxation rate from two 3D HNCO spectra (Chill et al. 2006). Whereas multidimensional experiments such as HNCO are routinely used to separate overlapping peaks and have previously been adapted to measure relaxation rates (Caffrey et al. 1998), full 3D spectra are not practical for measurements of relaxation rates due to the excessive time requirements. However, band-selective Hadamard frequency encoding allows the incorporation of carbonyl carbon (C′) chemical shift dispersion without the need to resolve fully the C′ dimension (Brutscher 2004). This, combined with the additive nature of the Hadamard matrix, produces much reduced resonance overlap without the need for an increase in the dimensionality of the experiment or a dramatic decrease in the signal to noise ratio. Hadamard encoding has previously been used as one of the methods for enabling fast NMR acquisition as has been reviewed in (Kupce et al. 2003). It has also been used to record NOE crosspeaks to methyl groups separated according to residue type (Van Melckebeke et al. 2004).

Here we present a suite of pulse sequences for the measurement of ^{15}N T_1, $T_{1\rho}$ and NOE which combine the traditional TROSY-based pulse sequences (Zhu et al.

Electronic supplementary material The online version of this article (doi:10.1007/s10858-007-9192-4) contains supplementary material, which is available to authorized users.

B. T. Burnley · A. P. Kalverda · S. J. Paisey · A. Berry · S. W. Homans (✉)
Astbury Centre for Structural Molecular Biology, University of Leeds, Leeds LS2 9JT, UK
e-mail: s.w.homans@leeds.ac.uk

2000) with a set of C′ band selective pulses (Brutscher 2004). The accuracy of relaxation measurements using these sequences has been validated using a sample of ^{2}H–^{15}N–^{13}C enriched ubiquitin and subsequently applied to *Escherichia coli* Class II fructose 1,6-bisphosphate aldolase (FBP-aldolase), a 358 residue 78 kDa dimeric enzyme.

Materials and methods

NMR measurements

Hadamard encoded relaxation sequences (Fig. 1) were validated against traditional TROSY based sequences (Zhu et al. 2000) using a 0.5 mM ^{2}H–^{15}N–^{13}C human ubiquitin sample (Prospect Pharma, Columbia, MD, USA). Four experiments were recorded with C′ shaped inversion pulses as follows: no inversion; inversion at greater than 176.4 ppm; inversion between 175.0–176.4 ppm and greater than 177.9 ppm; and inversion between 175.0 and 177.9 ppm. The C′ carrier was placed at 175.7 ppm. The inversions have different bandwidths and are chosen so that approximately equal numbers of peaks are sequestered in the four subspectra. However the boundaries of the inversion bands must be matched between the four experiments. As the sharpness of the inversion boundary depends on the strength of the shaped pulses, the optimum bandwidth and centre of the shaped pulses will not exactly coincide with the bandwidth and centre of the individual bands. We have optimized this by running a trial set of 2D experiments with chemical shift evolution in the C′ dimension and adjusting the bandwidth and centre of the shaped pulses for optimal correspondence of the frequency band boundaries. All data were collected using a 750 MHz Varian spectrometer equipped with a cold-probe. T_1 data were collected using the following delay times; 0, 80, 160, 320, 480, 720, 960, 1200 ms (where 80 and 720 ms were repeated for noise estimation). $T_{1\rho}$ data were collected using the following delay times; 0, 8, 12, 20, 32, 48, 64, 96 ms (where 12 and 64 ms were repeated for noise estimation). For the NOE saturation experiment the recycling delay was 5.5 s with proton saturation for 3.5 s. HSQC-TROSY relaxation experiments were acquired with four scans and spectral windows of 12,000 Hz and 3,200 Hz and 1,024 and 80 complex data points for the ^{1}H and ^{15}N dimensions, respectively. Hadamard relaxation experiments were acquired with the same spectral windows and number of points and with four scans per experimental spectrum (therefore effectively 16 scans after application of the Hadamard matrix). Relaxation rates for FBP-aldolase were measured with a 2.5 mM ^{2}H–^{15}N–^{13}C enriched sample. The following T_1 delay times were used: 0, 80, 160, 400, 800, 1440, 2640, 4480 ms and T_2 delay times were as follows 3, 4, 6, 9, 13, 18, 28, 48 ms. Two delay times were duplicated for spectral noise calculation, and 16 scans per experimental spectrum were recorded (therefore 64 effective scans per derived spectrum after application of Hadamard matrix). Other experimental parameters were as Hadamard encoded measurements on ubiquitin detailed above.

Data analysis

The spectra were recorded as interleaved FIDs. The spectral data were processed using NMRPipe software (Delaglio et al. 1995). A cosine bell function, followed by zero filling and Fourier transformation was used. Linear prediction was used in the ^{15}N dimension to double the number of points. Phase corrections were determined using the Fourier transformed one-dimensional slice and first 2D plane, which were examined with NMRDraw software (Delaglio et al. 1995) and inserted manually into a 2D phase correction macro. After processing of the direct dimension the individual spectra were separated and an NMRPipe (Delaglio et al. 1995) macro was used to perform the Hadamard subtraction matrix to convert the 2D experimental spectra to the final derived spectra used for relaxation rate analysis (further details are provided in supplementary information).

T_1 and T_2 rates were then calculated by measuring centered peak heights from eight spectra with varying delay times. Levenberg-Marquardt least-squares fitting to a two parameter exponential decay was used to determine relaxation rates from peak intensities. Rate errors were determined by 1000 Monte Carlo simulations. T_2 rates were calculated from experimental $T_{1\rho}$ measurements according to:

$$R1\rho = R2\cos^2\theta + R1\sin^2\theta \quad (1)$$

where $\tan\theta = (\Delta\omega/\gamma B_1)$, $\Delta\omega$ is the offset of a given ^{15}N resonance and B_1 is the strength of the spin-lock field. For the determination of the $^{15}N\{^{1}H\}$ NOE values, two spectra were collected, with and without proton saturation. The centered peak heights of the saturated resonance intensities were divided by the intensity of the corresponding non-proton saturated resonances. The standard deviation of noise from non-peak containing regions of spectra was used for error analysis.

In cases where the C′ chemical shift lies near the C′ band selection frequency it is possible that resonances are sequestered into multiple spectra. In these instances, rates in each spectrum were measured and, provided the fitting error was less than 50% of the rate, the rates (R) and associated errors (Δ R) were determined from:

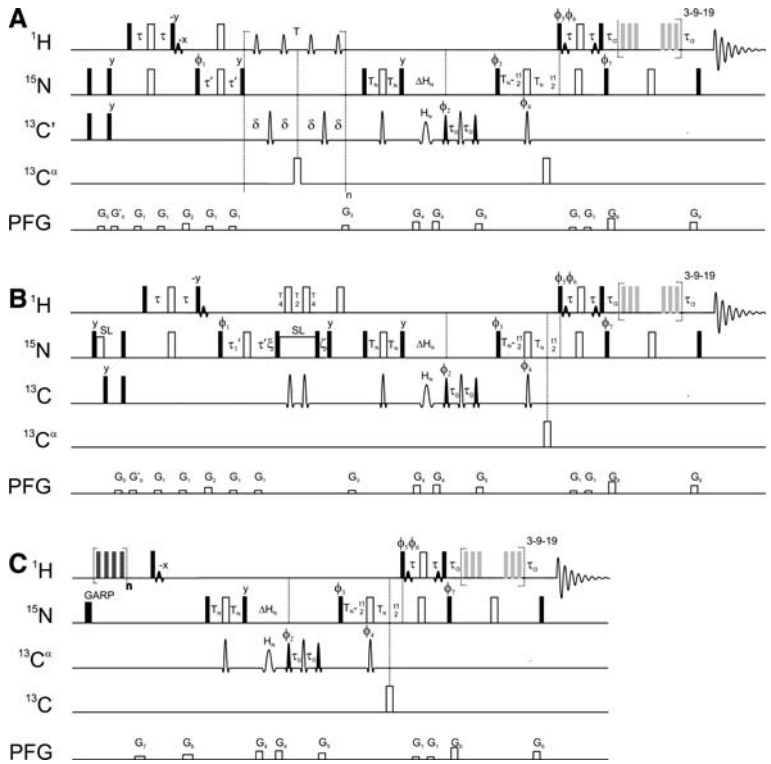

Fig. 1 Hadamard C′ encoded TROSY based pulse schemes for the measurement of ^{15}N T_1 (A), $T_{1\rho}$ (B) and NOE (C). Narrow (wide) pulses correspond to 90° (180°) flip angles with phase x, unless otherwise indicated. Water magnetization is placed along the + z-axis using flip-back pulses. The ^{13}C pulses applied to C′ have the shape of the center lobe of a (sin x)/x function, C^{α} pulses are applied off resonance with a rectangular shape and field strength adjusted to provide a null at C′. Nitrogen pulses are applied at a field strength of 5 kHz. The delays used are: τ = 2.25 ms, τ' = 2.75 ms, δ = 10 ms, T_N = 12.5 ms, ΔH_N = 20 ms, τ_0 = 10μs, τ_a = 1.93 ms, τ_b = 190μs, $\varepsilon = 1/(2\pi \times v1)$, $\xi = 1/(2\pi \times v1) - (4 \times pw)/\pi$, where v1 is the spin-lock field strength and pw is the width of the ^{15}N 90° pulse. Gradient amplitudes and durations (G/cm, ms) are: G_0, 5, 1; G_0', 4, 1; G_1, 5,0.5; G_2, 19, 1; G_3, 5, 1; G_4, 27.5, 1; G_5, 20, 1; G_6, 37.5, 1; G_7, 8, 0.4; G_8, 15, 0.4. For the Hadamard C′ encoding appropriate band selective inversion pulses H_N are applied according to a Hadamard matrix (Brutscher 2004). These used I-BURP2 pulse shapes and were generated using Pbox software (Varian, Inc., Palo Alto, CA). This generated the following inversion pulses using the center frequencies (bandwidths): 1, no inversion; 2, 179.6 ppm (5.8 ppm); 3, 175.5 ppm (1.25 ppm) and 180.3 ppm (4.3 ppm); 4, 176.3 ppm (2.5 pmm). For a minimal band width of 1.25 ppm the longest shape used was 19.7 ms. (**A**) Sequence for measuring ^{15}N longitudinal relaxation. The amide proton magnetization is inverted every 20 ms using a 330 μs rectangular 180° pulse in the T_1 relaxation period T with excitation maximum shifted 4 ppm downfield from the carrier. Phase cycling is as follows: $\varphi1$ = x,–x; $\varphi2$ = 4(x), 4(–x); $\varphi3$ = x,x,y,y; $\varphi4$ = x; $\varphi5$ = –y; $\varphi6$ = y; $\varphi7$ = –y; rec = y,–y,–x,x,–y,y,x,–x. Quadrature detection in ^{15}N is achieved by inverting $\varphi5$, $\varphi6$, $\varphi7$ and the receiver for every second fid and by setting $\varphi3$ = x,x,–y,–y. In addition $\varphi3$ and the receiver are inverted for every second increment. The data are processed in echo/antiecho fashion. (**B**) Pulse sequence for measuring ^{15}N $T_{1\rho}$. ^{15}N spin-lock field strength is 1.8 kHz. The applied radio frequency power is kept constant using a compensating ^{15}N spin-lock at the start of the sequence. ^{1}H and ^{13}C 180° pulses are applied at 1/4 and 3/4 of the spin-lock period (Massi et al. 2004). For ^{13}C, adiabatic inversion is used to cover both C^{α} and C′. (**C**) Pulse sequence for measuring $^{15}N\{^{1}H\}$ NOE. ^{1}H saturation is achieved with 120° pulses with a 5 ms interval for 3.5 s. 50 ms ^{15}N GARP decoupling is applied at the start of the sequence (Zhu et al. 2000). Phase cycling is as follows: $\varphi1$ = x,–x; $\varphi2$ = x,–x; $\varphi3$ = x,x,y,y; $\varphi4$ = x; $\varphi5$ = –y; $\varphi6$ = y; $\varphi7$ = –y; rec = y,–y,–x,x

$$R = \frac{\frac{1}{\sigma_1}}{\sum\frac{1}{\sigma}} r_1 + \frac{\frac{1}{\sigma_2}}{\sum\frac{1}{\sigma}} r_2 \ldots \frac{\frac{1}{\sigma_n}}{\sum\frac{1}{\sigma}} r_n \quad (2)$$

$$\Delta R = \frac{\sqrt{n}}{\sum\frac{1}{\sigma}} \quad (3)$$

where r_n is the rate from the individual sub-spectra, σ is the associated rate error from individual sub-spectra and n is the number of spectra in which a particular resonance is observed. Any resonance with a fitting error of greater than 50% of the rate value was discarded.

Results and discussion

Pulse sequences

In order to resolve overlapping peaks in the crowded ^{1}H–^{15}N spectra of large proteins a Hadamard style excitation is used in the C′ dimension. The resulting Hadamard C′ encoded TROSY based pulse sequences for measurement of ^{15}N T_1, $T_{1\rho}$ and NOE are shown in Fig. 1. The sequences are analogous to those utilized for conventional ^{15}N relaxation measurements (Farrow et al. 1994) until

after the variable time nitrogen relaxation delay. Subsequently magnetization is transferred via an INEPT pulse element to C′ where a series of shaped selective inversion pulses are applied. Then an HNCO-TROSY based detection scheme (Salzmann et al. 1998) is used without C′ chemical shift evolution, giving 2D ^{1}H-^{15}N spectra. The option of C′ chemical shift evolution is kept intact in the sequence, this is useful for calibration of the C′ inversions. Therefore the C′ magnetisation is briefly rotated to the transversal plane in similar fashion to the first increment of an HNCO experiment and resides there for $2\tau_0$ (20 μs). Solvent suppression is obtained using the Watergate method (Sklenar et al. 1993). The Hadamard frequency encoding is realized by dividing the spectrum into a set of frequency bands and using shaped pulses to invert these bands in one or more of the experiments. Linear combination of addition and subtraction of the resultant spectra gives the Hadamard encoded spectra. Spectra can be divided into N 2D sub-spectra for orders $N = 2^n$ or $N = 4n$ and the band selection frequencies can be calibrated for optimum peak dispersion in each sub-spectrum. Here, four frequency bands were chosen to cover the spectrum in the C′ dimension, as described in the methods section.

In a first series of experiments, the accuracy of measurements using these pulse sequences was validated using a ^{2}H–^{15}N–^{13}C ubiquitin sample. Residues 1, 16, 19, 23, 24, 26, 36, 37, 38, 39, 53, 58, 63, 71, 75, 76 were excluded from rate analysis because either they are prolines or the signal to noise ratio for the corresponding HSQC amide cross-peak was less than ten. Residue 1 is cleaved during protein expression. The relaxation rates measured for ubiquitin with traditional and Hadamard encoded pulse sequences and the percentage difference between the two measurements are shown in Fig. 2 and the data are collected in Table 1 (supplementary information). The RMSD of the percentage differences are 1.6%, 2.8% and 5.5% for T_1, T_2 and NOE experiments respectively and show no systematic bias. Thus the difference between the two

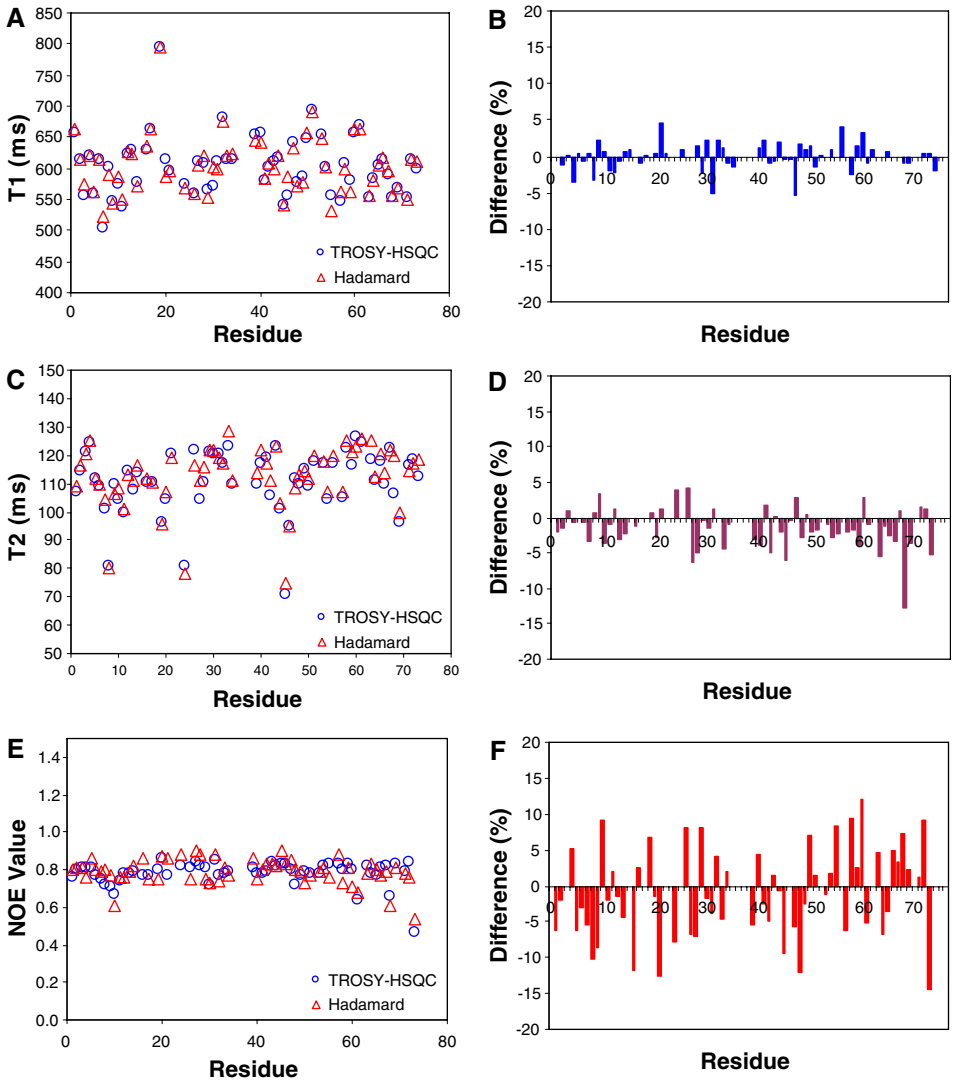

Fig. 2 Validation of Hadamard T_1, T_2 and NOE relaxation pulse sequences. Relaxation rates for [^{2}H, ^{13}C, ^{15}N]-ubiquitin from Hadamard encoded spectra are comparable with rates derived from standard 2D TROSY experiments (Zhu et al. 2000). (**A**) T_1 times and (**B**) percentage difference. (**C**) T_2 times and (**D**) percentage difference. (**E**) NOE values and (**F**) percentage difference. The measured relaxation rates are given in the supplementary information

methods of relaxation measurement is within experimental error.

Subsequently these methods were applied to relaxation-time measurements in *Escherichia coli* Class II fructose 1,6-bisphosphate aldolase (FBP-aldolase), a 358 residue 78 kDa dimeric enzyme. Class II FBP-aldolase catalyses the reversible aldol cleavage of fructose 1,6-bisphophate (FBP) into two trioses: dihydroxyacetone phosphate (DHAP) and glyceraldehyde 3-phosphate (Horecker 1972). It adopts the $(\alpha/\beta)_8$ barrel fold (Cooper et al. 1996), which is a common and versatile architecture, representing 10% of all known enzyme structures (Reardon and Farber 1995). Enzymes exhibiting an $(\alpha/\beta)_8$ barrel fold have been found for 61 different types of E.C. number, including all primary classes with the exception of ligases (Nagano et al. 2002). However, at present no high-resolution dynamic studies have been completed for such systems. This is due, in part, to the extensive peak overlap caused by the high helical content of such proteins. There are 206 amide cross-peaks present in the 3D HNCO spectrum of ^{2}H–^{15}N–^{13}C FBP-aldolase which have a signal to noise ratio greater than three. Of these only 38% (78 cross-peaks) can be unambiguously isolated in the corresponding 2D TROSY spectrum (judged using standard criteria (Tugarinov et al. 2004)). The extensive cross peak overlap, particularly in the central portion of the spectrum, present in the traditional TROSY-type relaxation experiments can be seen in Fig. 3A. As such, a complete analysis of conformational dynamics for this protein is critically impaired using standard techniques. When Hadamard encoding is applied (Fig. 3B–E), cross-peaks are sequestered into four sub-spectra, dramatically reducing resonance overlap. This allows the independent measurement of 79% (162) of the cross-peaks, over twice the number previously measurable. The T_1 and T_2 (derived from the $T_{1\rho}$ experiment) rates have been measured for FBP-aldolase and are reported in Table 2 (supplementary information). This reveals a mean T_1 and T_2 of 1950± 30 ms and 20± 0.6 ms respectively, corresponding to a calculated τ_c of 35± 1 ns using the method of Tjandra et al. (1995). Although resonance assignments have not been confirmed at present, these data reveal high variance in the sub-nanosecond dynamics of the peptide backbone which may be functionally related. Figure 4 illustrates a cluster of four overlapped cross-peaks which are sequestered into different Hadamard sub-spectra. Without Hadamard encoding only one (peak number 1) of the four overlapped cross-peaks can be measured using TROSY based spectra. When Hadamard encoding is used the relaxation rates for each of these resonances can be independently measured. Some cross-peaks appear in multiple spectra (see peaks 1 and 3 in Fig. 4) if the C′ chemical shift is near a band selection frequency boundary. When this occurs measurements are taken from each spectrum and averaged using an error weighted algorithm (see methods).

Two issues affect the reduction of artifacts and clean separation of signals into the different subspectra. First, this depends upon how well matched the boundaries of the inversion bands are between the experiments employing different inversion pulses. This can be optimized with a trial experiment as described in methods. Second, peak intensities in the individually recorded experiments must be the same within experimental error for the linear combination to be effective. In principle differences in peak intensities could arise from differential relaxation between band selective pulses of different lengths. In this regard IBURP2 is a good choice for the shaped inversion pulses as the magnetization remains close to the z-axis for the majority of the pulse trajectory. For an IBURP2 shaped pulse the effect of relaxation of the transversal components

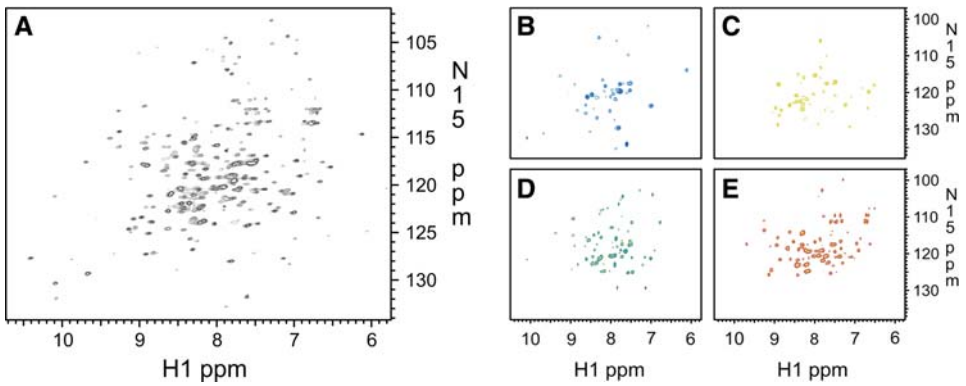

Fig. 3 TROSY and C′ encoded Hadamard spectra of the *E.coli* Class II fructose-1,6-bisphophate aldolase. (**A**) TROSY spectrum displaying the extensive cross-peak overlap with only 40% of the amide resonances detected in the HNCO spectra (not shown) being suitable for relaxation rate measurement. (**B**–**E**) Spectra derived from Hadamard-TROSY pulse sequences exhibit significantly improved peak dispersion allowing the measurement of ~ 80% of visible peaks. Spectra were acquired with a 750 MHz spectrometer with a cold-probe

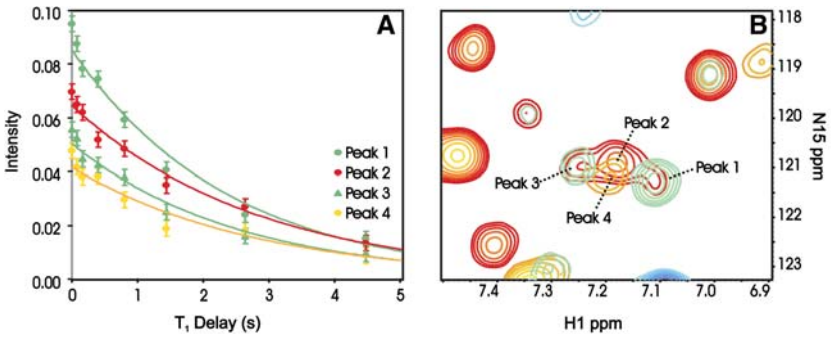

Fig. 4 Measurement of T_1 relaxation rates from overlapping amide cross-peaks in *E.coli* Class II fructose-1,6-bisphophate aldolase. (**A**) T_1 relaxation rates for the four selected peaks. (**B**) Section of a Hadamard-TROSY spectrum with the four derived sub-spectra (blue, green, red, and orange) overlaid. The sequestering of cross-peaks into the Hadamard spectra allows unambiguous rate measurement

during the pulse has been estimated as equivalent to transverse relaxation being present for 14.2% of the duration of the shaped pulse (Hajduk et al. 1993). This indicates that relaxation during the shaped inversion pulses is minor even for a protein the size of FBP-aldolase as long as the duration of the shaped pulses is kept reasonably short. In our current application inversion bandwidths varied from 5.8 ppm to 1.25 ppm, leading to the duration of the various shaped pulses varying between 4.27 ms and 19.7 ms, and no significant differences in intensity were found between subspectra recorded with different inversion bands. The differential relaxation between band selective pulses of different lengths will however need to be taken into account when much smaller bandwidths are used. It can be accounted for by adjusting the length of the τ_0 delay to compensate for differential relaxation between the experiments. Very long inversion pulses ($\gg$20 ms) will however lower the sensitivity of the experiment.

Conclusions

C′ band selection is an efficient method for decreasing resonance overlap as backbone amide nitrogen and C′ chemical shifts are not correlated. Despite the additional magnetization transfer step, the inversion pulses do not require a C′ chemical shift evolution and as such signal-to-noise is not dramatically reduced. In comparison with traditional HSQC-TROSY relaxation experiments, the signal-to-noise ratio is reduced by a factor of 1.8 for ubiquitin, (recorded at 25°C, 750 MHz) and 2.6 for FBP-aldolase (also recorded at 25°C, 750 MHz). Unlike alternative methods such as tilted plane projections where a series of discrete spectra are recorded (Tugarinov et al. 2004) the Hadamard approach allows all peaks to be simultaneously measured in each experiment thus maximizing signal to noise per unit time. Other pulse sequences used for quantitative measurements of protein structure and dynamics, such as relaxation dispersion or residual dipolar couplings, could also be adapted in a similar manner (Brutscher 2004). This suite of pulse sequences offers a simple and efficient method of peak separation in large protein systems in combination with quantitative measurement of sub-nanosecond dynamic motion. It is hoped this will further stimulate the investigation of large biomolecules by NMR.

Acknowledgments This work was funded by the BBSRC, U.K., grant number BBS/B/05680.

References

Brutscher B (2004) Combined frequency- and time-domain NMR spectroscopy. Application to fast protein resonance assignment. J Biomol NMR 29:57–64

Caffrey M, Kaufman J, Stahl SJ, Wingfield PT, Gronenborn AM, Clore GM (1998) 3D NMR experiments for measuring 15N relaxation data of large proteins: application to the 44 kDa ectodomain of SIV gp41. J Mag Res 135:368–372

Chill JH, Louis JM, Baber JL, Bax A (2006) Measurement of 15N relaxation in the detergent-solubilized tetrameric KcsA potassium channel. J Biomol NMR 36:123–36

Cooper SJ, Leonard GA, McSweeney SM, Thompson AW, Naismith JH, Qamar S, Plater A, Berry A, Hunter WN (1996) The crystal structure of a class II fructose-1,6-bisphosphate aldolase shows a novel binuclear metal-binding active site embedded in a familiar fold. Structure 4:1303–1315

Delaglio F, Grzesiek S, Vuister GW, Zhu G, Pfeifer J, Bax A (1995) NMRPipe: a multidimensional spectral processing system based on UNIX pipes. J Biomol NMR 6:277–293

Eisenmesser EZ, Millet O, Labeikovsky W, Korzhnev DM, Wolf-Watz M, Bosco DA, Skalicky JJ, Kay LE, Kern D (2005) Intrinsic dynamics of an enzyme underlies catalysis. Nature 438:117–121

Farrow NA, Muhandiram R, Singer AU, Pascal SM, Kay CM, Gish G, Shoelson SE, Pawson T, Forman-Kay JD, Kay LE (1994). Backbone dynamics of a free and phosphopeptide-complexed Src homology 2 domain studied by 15N NMR relaxation. Biochemistry 33:5984–6003

Hajduk PJ, Horita DA, Lerner LE (1993) Theoretical analysis of relaxation during shaped pulses I. The effects of short T1 and T2. J Mag Res A 103:40

Horecker BL, Tsolas O, Lai CY (1972) The enzymes. Academic Press, New York, USA

Jarymowycz VA, Stone MJ (2006) Fast time scale dynamics of protein backbones: NMR relaxation methods, applications, and functional consequences. Chem Rev 106:1624–1671

Kupce E, Nishida T, Freeman R (2003) Hadamard NMR spectroscopy. Prog NMR Spec 42:95

Massi F, Johnson E, Wang C, Rance M, Palmer AG 3rd (2004) NMR R1 rho rotating-frame relaxation with weak radio frequency fields. J Am Chem Soc 126:2247–2256

Nagano N, Orengo CA, Thornton JM (2002) One fold with many functions: the evolutionary relationships between TIM barrel families based on their sequences, structures and functions. J Mol Biol 321:741–765

Pervushin K, Riek R, Wider G, Wuthrich K (1997) Attenuated T2 relaxation by mutual cancellation of dipole-dipole coupling and chemical shift anisotropy indicates an avenue to NMR structures of very large biological macromolecules in solution. Proc Natl Acad Sci USA 94:12366–12371

Reardon D, Farber GK (1995) The structure and evolution of alpha/beta barrel proteins. FASEB J 9:497–503

Salzmann M, Pervushin K, Wider G, Senn H, Wuthrich K (1998) TROSY in triple-resonance experiments: new perspectives for sequential NMR assignment of large proteins. Proc Natl Acad Sci USA 95:13585–13590

Sklenar V, Piotto M, Leppik R, Saudek V (1993) Gradient-Tailored Water Suppression for ^{1}H-^{15}N HSQC Experiments Optimized to Retain Full Sensitivity. J Mag Res A 102:241–245

Tjandra N, Feller SE, Pastor RW, Bax A (1995) Rotational diffusion anisotropy of human ubiquitin from 15N NMR relaxation. J Am Chem Soc 117:12562–12566

Tugarinov V, Choy WY, Kupce E, Kay LE (2004) Addressing the overlap problem in the quantitative analysis of two dimensional NMR spectra: application to (15)N relaxation measurements. J Biomol NMR 30:347–352

Van Melckebeke H, Simorre J, Brutscher B (2004) Amino acid-type edited NMR experiments for methyl-methyl distance measurement in 13C-labeled proteins. J Am Chem Soc 126:9584–9591

Venters RA, Farmer Ii BT, Fierke CA, Spicer LD (1996) Characterizing the use of perdeuteration in NMR studies of large proteins:13C,15N and1H assignments of human carbonic anhydrase II. J Mol Biol 264:1101

Zhu G, Xia Y, Nicholson LK, Sze KH (2000) Protein dynamics measurements by TROSY-based NMR experiments. J Mag Res 143:423–426